Вісник Астрономічної школи | Astronomical School's Report

ISSN 1607–2855

Том 9 • № 2 • 2013 С. 142 – 145

UDC 524.7

Multiwavelength studies of extragalactic jets structure

A.V. Bogdan[1], **V.V. Marchenko**[2], **B.I. Hnatyk**[1]

[1]Taras Shevchenko National University of Kyiv, Astronomical Observatory

[2]Taras Shevchenko National Pedagogical University of Chernihiv, Astronomical Scientific Research Center

This research is devoted to the analysis of extragalactic jets structure using the multiwavelength data. We analyze the core-dominated quasar 3C 273 using the Chandra, HST and VLA data. The attempt to resolve the perpendicular jet structure is made. The data in X-ray, UV and radio wavebands are used to compare jet structure in different wavelengths.

МУЛЬТИХВИЛЬОВЕ ДОСЛІДЖЕННЯ СТРУКТУРИ ПОЗАГАЛАКТИЧНИХ ДЖЕТІВ, Богдан А.В., Марченко В.В., Гнатик Б.І. — Ця стаття присвячена аналізу структури позагалактичних джетів з використанням даних різних довжин хвиль. Ми аналізуємо структуру джету квазара 3C 273 використовуючи дані Chandra, HST и VLA. Було проведено аналіз та порівняння поперечної складової вузлів джету в рентгенівському, ультрафіолетовому та радіодіапазонах.

МУЛЬТИВОЛНОВОЕ ИССЛЕДОВАНИЕ СТРУКТУРЫ ВНЕГАЛАКТИЧЕСКИХ ДЖЕТОВ, Богдан А.В., Марченко В.В., Гнатык Б.И. — Эта статья посвящена анализу структуры внегалактических джетов с использованием данных различных длин волн. Мы анализируем структуру джета квазара 3C 273 используя данные Chandra, HST и VLA. Был проведен анализ и сравнение поперечной составляющей узлов джета в рентгеновском, ультрафиолетовом и радиодиапазонах.

Ключевые слова: квазары; джеты; рентгеновское, ультрафиолетое и радио излучение.

Key words: quasars; jets; X-ray, UV and radio emission.

1. INTRODUCTION

The active galactic nuclei (AGN) are one of the most interesting and remarkable objects for modern astrophysics [1]. It's generally accepted that the AGN jets are powered by central supermassive black holes activity and this leads to the fact, that AGN jets are the longest collimated structures in the Universe [2]. The analysis of extragalactic jets structure in different wavelengths is an important task for modeling the different astrophysical processes that take place in jets, like acceleration of cosmic rays and the related time varying emission processes.

In this article we compare the actual size of the jet in different wavelengths, namely, radio, ultraviolet (UV) and X-ray bands. Each energy band indicates about particles with different energy in the jet and analysis of this regions help as to understand dynamic of jet.

In view of the fact that any resulting image is the result of a convolution of the real image with point spread function (PSF) of a given telescope, the primary goal of our study was to restore the image of the real jet. The importance of this procedure highly increases, if one take into account the fact, that the size of knots in X-ray is comparable with the PSF size. This problem is solved simply enough for the radio and UV, while for X-rays, this task is much more difficult because the PSF size is comparable to the size of the knot. In our study, we used the radio data from VLA, UV data from Hubble Space Telescope and X-ray data from Chandra X-ray Observatory. It would be more interesting to see the structure of the jet in the gamma range, but unfortunately the resolution of the gamma-ray telescopes is not enough high to see the jet of the quasar 3C 273.

2. OBSERVATION DATA AND POINT SPREAD FUNCTION

2.1. X-ray data

Six Chandra observations of the core-dominated quasar 3C 273 and its jet are analyzed: four dedicated observations (ObsIDs: 4876, 4877, 4878, 4879) with total exposure time of 160 ks [3] and two Chandra calibration observations (ObsIDs: 1711, 1712) with the total exposure time of 56 ks. The merged data have binned with binning factor of 0.125, that corresponds to the bin size of 0.0615″ (Fig. 1).

The X-ray data analysis was processed with CIAO 4.5 — a software package for Chandra interactive analysis of observations [7] and CALDB 4.5.6. Before analysis we reprocessed the data using *chandra_repro* reprocessing script that makes all recommended data processing steps presented in the CIAO analysis threads. The pixel randomization was removed during reprocessing.

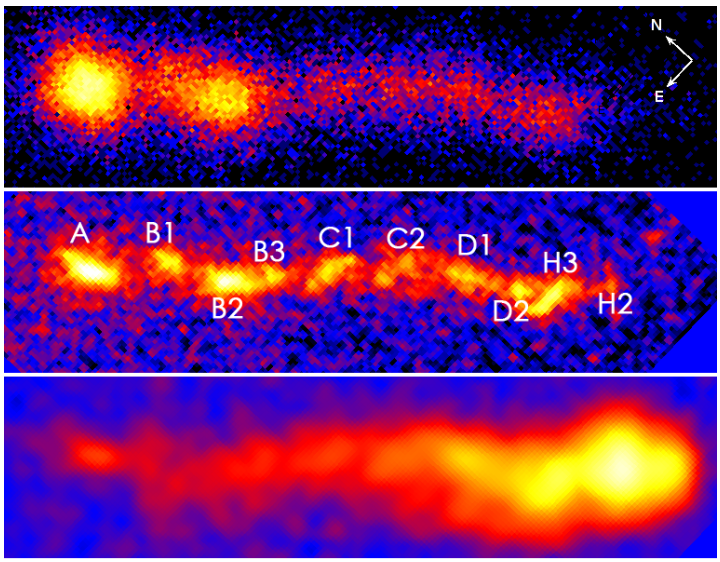

Fig. 1. The Chandra X-ray (top) [3], Hubble ACS/SBC ultraviolet (middle) [4] and VLA radio images of 3C 273 jet at 8.4149 GHz (bottom) [5]. Size of bin is $0.0615'' \times 0.0615''$.

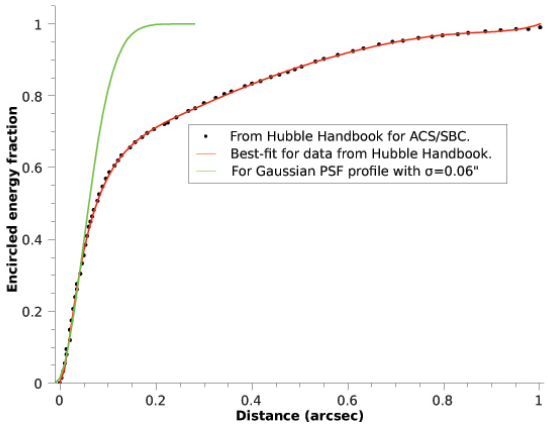

Fig. 2. Encircled energy for the Hubble ACS/SBC.

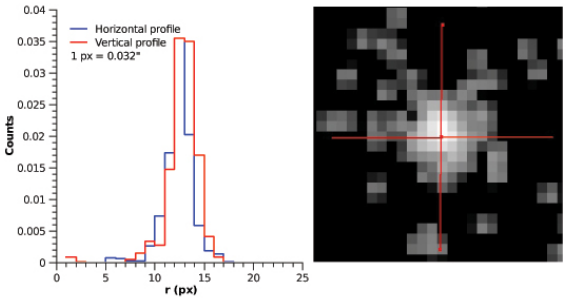

Fig. 3. Image of UV star (right) and different profiles for this star (left) in original pixel size (1 px = 0.032").

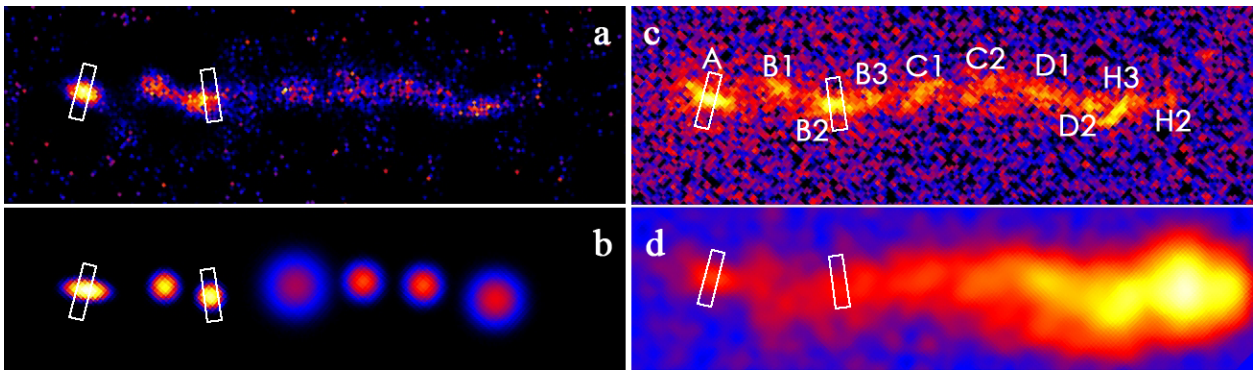

Fig. 4. Restored data: X-ray data restored by forward-fitting algorithm (a), X-ray data restored by Lucy-Richardson deconvolution algorithm (b), UV data restored by Lucy-Richardson deconvolution algorithm (c). Radio data (d). White boxes indicate regions of knots A and B2 which were used for analysis. Size of bin is $0.0615'' \times 0.0615''$.

To proceed detailed ray-trace simulation and get the best available Chandra PSF we used the combination of ChaRT [8] and MARX [9]. The "spectrum & exposure time" spectral specification were used in ChaRT for modeling the ACIS PSF [10]. The source spectrum for modeling ACIS PSF was used with subtracted background in the energy range $0.4-8.0$ keV including Galactic absorption $N_H = 1.71 \cdot 10^{20}$ atoms/cm^2 and fitted using Sherpa [11].

2.2. Hubble ACS/SBC Point Spread Function

The HST far-ultraviolet observations at ∼150 nm of the 3C 273 jet were obtained with the Advanced Camera for Surveys (ACS) Solar Blind Channel onboard the Hubble Space Telescope [4] (Fig. 1 and Table 1).

Table 1. Observation log for analyzed ACS/SBC data. All data used the filter `F150LP`.

Target	Dataset name	Start time, UT	Exp. time, s
J122903+020318	J8P001010	04/08/2004 23:13:47	900
3C273-JET	J8P001TSQ	04/08/2004 23:32:12	1600
3C273-JET	J8P001020	05/08/2004 00:45:39	2800
3C273-JET	J8P001030	05/08/2004 02:21:37	2800

To estimate the PSF for ACS/SBC data several attempts were made. At first the encircled energy fraction from Hubble Handbook for ACS/SBC were analyzed. Using the ACS Instrument Handbook for Cycle 12 [6] one can find the encircled energy fraction for the ACS/SBC generated from data acquired during the servicing mission orbital verification (Fig. 2 and also Figure 4.11 and comments in [6]).

In order to restore the PSF profile we have fitted the ACS/SBC encircled energy distribution (Figure 2) and reproduce the PSF profile from that fitted curve, taking into account the relationship between the encircled energy distribution $\nu(r)$ and PSF profile $f(r)$.

We have checked different functions for PSF (Figure 2). According to Hubble encircled energy fraction distribution the PSF profile can be described by Gaussian only in central region of PSF (up to 0.05″) but the wings of PSF is not Gaussian (see Figure 2). We have figured out that the better fit for PSF profile is with Lorentz function $F(r)$ but still with some deviations from curve. In order to improve the fit we add the polynomial function to Lorentz and finally obtained equation for $f(r)$, that hereafter use for creating the FITS-file of UV PSF (Figure 2).

One more attempt to find the PSF for ACS/SBC was made using the image of a distant point source from exactly the same dataset as for 3C 273. We have used as such object an image of normal star from dataset J8P001010 (see Table 1), that the authors tried to use for astrometry calibration [4]. The image of UV star have been found to be quite consistent with the PSF, obtained from ACS/SBC encircled energy distribution.

2.3. Radio data

The radio data were obtained by VLA at 8.4149 GHz in 1995. The data was already deconvolved with the Gaussian PSF, the parameters of which is listed in a Table 2.

Table 2. The radio data observed by VLA at 8.4149 GHz in 1995.

Generic Name	z	Class[1]	Pixel size (″/px)	BMAJ[2] (″)	BMIN[3] (″)	BPA[4] (deg)
3C 273	0.1583	CDQ	0.075	0.35	0.35	0

[1] CDQ = Core-Dominated Quasar;
[2] The major axis of a beam (FWHM);
[3] The minor axis of a beam (FWHM);
[4] The position angle of a beam measured from N through E.

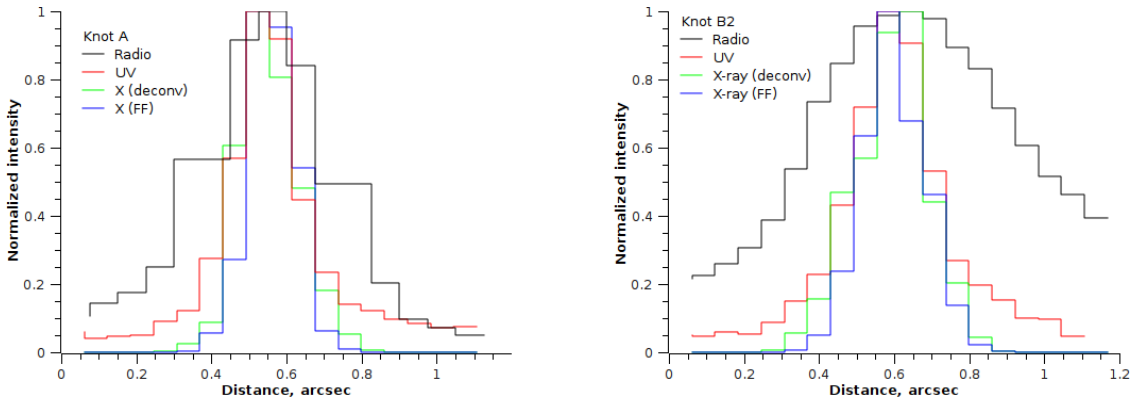

Fig. 5. The transverse sizes of the knots A and B2 in X-ray, UV and radio wavebands. The X-ray is recovered using LR deconvolution and forward-fitting procedures, UV data is a result of LR deconvolution and radio data were also deconvolved in AIPS (add reference for radio data). On the insert the considered regions are shown.

3. RESULTS AND CONCLUSIONS

The two brightest knots A and B2 were taken for analysis. The transverse sizes of these knots in X-ray, UV and radio wavebands were estimated. Different techniques were used for restoring the X-ray image, namely the forward-fitting [13] and Lucy-Richardson deconvolution [12] algorithms (Fig. 4 a,b). The UV image was recovered by Lucy-Richardson deconvolution algorithm (Fig. 4 c).

One can notice from obtained profiles for knots A and B2 (Fig. 5), that X-ray transverse profiles obtained from two different methods (forward-fitting and Lucy-Richardson deconvolution) are in good correspondence. The radio size of knots is significantly wider then X-ray and UV, while X-ray and UV knots have comparable sizes in the central part of jet. But the outer part of UV knots seems to be wider then correspondent X-ray knot.

A detailed study of extragalactic jets structure in all wavelengths is an important task for modeling the different astrophysical processes that take place in jets. These results can be used for future analysis of emission processes in relativistic jets and cosmic ray acceleration mechanisms in AGN. Taking into account, that knowledge of geometrical size of acceleration region can lead us to a possibility to estimate the different characteristics of particles and surrounding medium (e.g. the upper limit for parameters of accelerated particles, the values and structure of magnetic fields etc), one can conclude that analysis of AGN jet structure are of high importance and actuality.

Acknowledgments. The authors acknowledge to Michal Ostrowski (Astronomical Observatory of Jagiellonian University, Poland), Lukasz Stawarz (Japan Aerospace Exploration Agency, Japan) and Dan Harris (Harvard-Smithsonian Center for Astrophysics, USA) for assistance and fruitful discussions.

1. *Comastri A., Brusa M.* // Astronomische Nachrichten. — 2008. — **329**. — P. 122.
2. *Harris D.E., Massaro F., Cheung C.C.* // AIP Conference Proceedings. — 2010. — 1248, 355
3. *Jester S., et al.* // The Astrophysical Journal. — 2006. — **648**. — P. 900.
4. *Jester S., et al.* // Monthly Notices of the Royal Astronomical Society. — 2007. — **380**. — P. 828
5. *Roser H.-J., Conway R.G., Meisenheimer K.* // Astron. Astroph. — 1996. — **314**. — P. 414.
6. ACS Point Spread Functions: http://documents.stsci.edu/hst/acs/documents/handbooks/cycle12/c04_imaging8.html
7. *Fruscione A., et al.* // 2007, Chandra Newsletter, 14, 36
8. *Carter C., et al.* // ADASS XII ASP Conference Series, 295, 477
9. *Wise M.W., et al.* // A.S.P. Conference Series. — 1997. — **125**. — P. 477.
10. Preparing to Run ChaRT: http://cxc.cfa.harvard.edu/chart/threads/prep/
11. *Freeman P., et al.* // SPIE Conference 4477: Astronomical Data Analysis, San Diego, CA, July 2001.
12. *Bogdan A.V., Marchenko V.V., Hnatyk B.I.* The structure of X-ray jet of 3C 273 // Astronomical Schools Report. — 2012. — **8**, № 1–2. — P. 55–57.
13. *Bogdan A., Marchenko V., Hnatyk B.* X-ray structure of extragalactic jets // Bulletin of Taras Shevchenko National University of Kiev. Series: Astronomy (in press).

Received 11.11.2013